

Research Article

Plate tectonics and the origin of the Juan Fernández Ridge: analysis of bathymetry and magnetic patterns

Cristián Rodrigo¹ & Luis E. Lara²

¹Facultad de Ingeniería-Geología, Universidad Andrés Bello, Quillota 980, Viña del Mar, Chile

²Servicio Nacional de Geología y Minería, Avenida Santa María 0104, Santiago, Chile

ABSTRACT. Juan Fernández Ridge (JFR) is a *ca.* 800 km long alignment of seamounts and islands which is thought to be fed by a deep mantle plume. JFR includes the Friday and Domingo seamounts in the western active edge close to the active hotspot, and the O’Higgins Seamount and Guyot at the eastern limit just in front of the Chile-Perú trench. Recent bathymetric (Global Topography) and magnetic (EMAG-2) datasets were interpreted both qualitatively and quantitatively by means of 3D inverse modeling and 2D direct modeling for geometry and susceptibility, together with an interpretation of the synthetic anomalies related to the classical hypothesis of deep seafloor spreading. Topographic and magnetic patterns are used to understand the tectonic evolution and origin of the JFR, especially in the western segment. Results show a continuous corridor with a base at ~3900 m depth formed by four groups of seamounts/islands with a number of summits. The deep ocean floor is ~22 to ~37 Myr old and is younger to the south of the Challenger Fracture Zone that runs in a SW-NE direction. The magnetic pattern of the western JFR segment, which is different than the eastern one, has no correlation with bathymetry and does not present a common polarity nor fit with magnetic models for isolated bodies. This superposition of magnetic patterns indicates a role of the faults/fractures of the Nazca Plate. Geological evidence supports the hypothesis of a fixed mantle plume for the origin of JFR but our data suggest that tectonic processes play a role, thus fueling the global controversy about these competing processes.

Keywords: seamounts, hotspots, magnetic anomalies, bathymetry, Juan Fernández Ridge.

Tectónica de placas y origen de la dorsal de Juan Fernández: análisis de los patrones batimétricos y magnéticos

RESUMEN. El cordón o dorsal de Juan Fernández (JFR) es un alineamiento de montes submarinos e islas supuestamente asociadas a la actividad de una pluma mantélica. Comprende, por el W, desde los montes submarinos Friday y Domingo, cercanos al actual ‘hotspot’, y por el oeste, el guyot y monte O’Higgins cercanos a la fosa submarina de Chile-Perú, con una extensión total de *ca.* 800 km y un rumbo de ~N80°E. Compilaciones recientes de datos batimétricos (Global Topography) y magnéticos (EMAG-2), se interpretaron cualitativa y cuantitativamente a través de la generación de modelos de magnetización 3D por modelado inverso, y de geometría y susceptibilidad en una sección 2D por modelado directo, complementado con la interpretación de anomalías sintéticas generadas según la hipótesis clásica de la expansión del piso marino profundo. Se utilizan patrones topográficos y magnéticos para comprender la evolución tectónica y el origen del cordón, particularmente en su segmento occidental. Los resultados muestran que en el área de estudio el cordón genera una alineamiento continuo a ~3900 m de profundidad, conformado por cuatro grupos de montes o islas con varias cumbres individuales. El piso marino profundo tiene una edad que fluctúa de ~22 a ~37 Ma, siendo más joven hacia el sur de la Zona de Fractura Challenger que se extiende en dirección SW-NE. El patrón magnético del segmento occidental del cordón, que es diferente al del este, no tiene correlación con la batimetría, no presenta una polaridad común, ni se ajusta a modelos magnéticos de cuerpos aislados. Esta superposición de patrones magnéticos indicaría un rol de las fallas/fracturas de la placa de Nazca. La evidencia geológica apoya la hipótesis de una pluma fija del manto para el origen de la dorsal, pero nuestros datos sugieren que los procesos tectónicos juegan un cierto rol, alimentando así la controversia global acerca de estos procesos en competencia.

Palabras clave: montes submarinos, punto caliente, anomalías magnéticas, batimetría, dorsal Juan Fernández.

INTRODUCTION

Juan Fernández Ridge (JFR) is an aseismic ridge formed by an aseismic chain of seamounts and islands that includes the Friday (Farley *et al.*, 1993) and Domingo (Devey *et al.*, 2003) seamounts at the western edge, and the O'Higgins guyot (Vergara & Morales, 1985) close to the Chile-Perú trench, with a total length of ~800 km (Fig. 1) striking ~80°E at ~33.4°S. Geophysical evidence suggests extension of the JFR beyond the trench (*e.g.*, Papudo seamount; Von Huene *et al.*, 1997; Yáñez *et al.*, 2001) with related forearc deformation and intraplate seismicity (Von Huene *et al.*, 1997; Yáñez *et al.*, 2002).

The only emerged lands of the JFR form the Juan Fernández Archipelago, which is composed of Robinson Crusoe, Santa Clara and Alejandro Selkirk islands and a number of minor islets that produce a singular oceanographic setting and provide favorable conditions for endemic flora and fauna (Arana, 1985, 2010). As for other seamounts worldwide (*e.g.*, Clark *et al.*, 2010), the significant height of these seamounts also provides unique biological conditions (*e.g.*, Andrade & Pequeño, 2008).

Global relief and roughness of the sea floor is thought to be a result of tectonic and magmatic processes at the oceanic lithosphere (*e.g.*, Becker *et al.*, 2009). Seamounts are a result of intraplate volcanism, which can be fed from deep mantle plumes or the upper mantle through lithosphere structures (Courtillot *et al.*, 2003). Former hypotheses suggested hotspot volcanism as related to fixed mantle plumes (Wilson, 1965; Morgan, 1971) or hotlines (Bonatti *et al.*, 1977), probably related to fracture zones in the overlying crust (*e.g.*, Batiza, 1982). In general, some key features of ocean islands are compatible with fixed mantle plumes (*e.g.*, Steinberger, 2000; Davies & Davies, 2009), mostly for their age progression, high buoyancy flux and high $^3\text{He}/^4\text{He}$ (Courtillot *et al.*, 2003 and references therein). However, there is a wide typology of ocean islands and seamounts, some of them with no clear age progression as shown for the Pacific basin by Clouard & Bonneville (2001). Those called tertiary hotspots (Courtillot *et al.*, 2003) would be related to upper crustal processes as extensional fractures (Bonatti *et al.*, 1977; Koppers *et al.*, 2003; Koppers & Watts, 2010). The plume hypothesis has been challenged by Foulger (2011) who claims that plate tectonic processes play a major role in hotspot volcanism, and by Anderson (2013) who claims mantle plumes are basically a well-established myth.

On the other hand, the location of the active hotspot at JFR has been a matter of discussion, though it should be west of Alejandro Selkirk Island (*e.g.*, Von Huene *et al.*, 1997) and probably close to the Domingo Seamount (Devey *et al.*, 2003). Here we perform an analysis of bathymetric and magnetic data from public sources aimed to identify patterns that allow a better understanding of the origin and evolution of the western segment of JFR (the eastern segment has been characterized in previous works by Von Huene *et al.*, 1997; Yáñez *et al.*, 2001, 2002; Kopp *et al.*, 2004), and the possible role of plate tectonic processes as an explanation for the magmatic features along the JFR.

al., 1997) and probably close to the Domingo Seamount (Devey *et al.*, 2003). Here we perform an analysis of bathymetric and magnetic data from public sources aimed to identify patterns that allow a better understanding of the origin and evolution of the western segment of JFR (the eastern segment has been characterized in previous works by Von Huene *et al.*, 1997; Yáñez *et al.*, 2001, 2002; Kopp *et al.*, 2004), and the possible role of plate tectonic processes as an explanation for the magmatic features along the JFR.

GEODYNAMICS AND TECTONIC SETTING

JFR is located in the eastern Pacific where the Nazca Plate converges against the South American margin and is the most prominent feature at this latitude (Fig. 1). There is not a mirror structure to the west of the East Pacific Rise (Pilger, 1981). The Nazca Plate obliquely sinks beneath the South American plate at a long-term convergence rate of 8.5 cm yr⁻¹ (DeMets *et al.*, 1994). The effect of the indenter represented by the JFR is evident in the Valparaíso basin where a thicker crust is inferred from the gravimetric anomaly (Von Huene *et al.*, 1997; Yáñez *et al.*, 2001).

Along with the magnetic imprint, plate structures at the Challenger Fracture Zone could be playing a role in the evolution of JFR (Fig. 1). This fracture is close to the Chile Fracture Zone, which begins at the Chile Ridge at ~36°S (for a comprehensive review of the sea floor fabric the reader is referred to Matthews *et al.*, 2011). The Challenger Fracture Zone changes its strike from W-E at the Chile Ridge to a more oblique E-NE when approaching the continental margin. This change occurs to the east of the Selkirk trough (Fig. 1). The latter could be a pseudofault of a propagating ridge (*e.g.*, Tebbens & Cande, 1997) generated during the isochrone 6C (~24 Myr; Handschumacher, 1976; Hey, 1977) when a plate reorganization occurred as inferred from the analysis of magnetic anomalies (Mammerickx & Klitgord, 1982). The Crusoe basin formed at the isochrones 5A (~12 Myr) when crust was transferred to the Antarctic plate resulting in a northward migration of the triple junction Pacific-Antarctica-Nazca (Tebbens & Cande, 1997). As a result, a number of propagating ridges and microplates formed and disappeared. The Selkirk basin is related to the fossil Selkirk microplate (Blais *et al.*, 2002) and the Crusoe trough is related with the Friday microplate (Tebbens *et al.*, 1997) and all of them define the structural fabric of the sea floor surrounding the western segment of JFR.

MATERIALS AND METHODS

Bathymetry

Global Topography version 15.1 released in 2012 (Smith & Sandwell, 1997) was used as a primary source

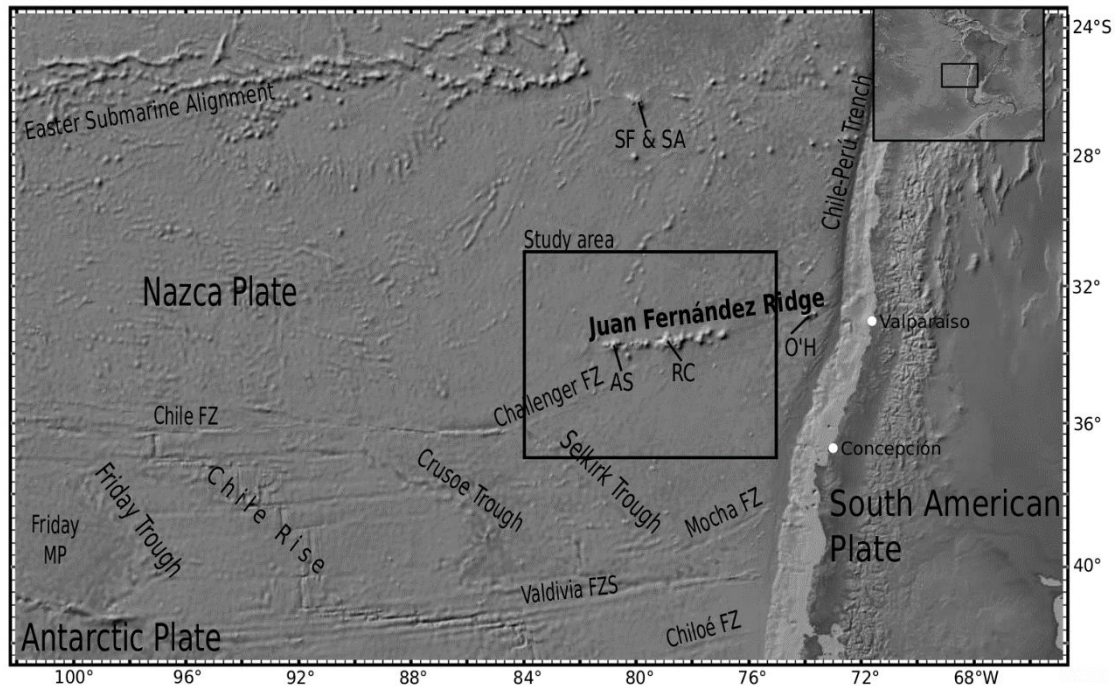


Figure 1. Map of the regional topography that includes global bathymetry (Global Topography 15.1). San Félix (SF), San Ambrosio (SA), Alejandro Selkirk (AS) and Robinson Crusoe (RC) islands. The study area and the main structures are shown (FZ: Fracture Zone, FZS: Fracture Zone System, MP: microplate).

for bathymetric data. This grid has a resolution of 1' arc (~ 1.8 km) and comprises satellite altimetry and data from single and multibeam bathymetry. Cruise tracks were extracted from the U.S. National Geophysical Data Center (www.ngdc.noaa.gov) and used to check the Global Topography grid. A better resolution grid (0.12' arc) was prepared only with the multibeam bathymetry.

Magnetic data

As occurred with bathymetry, magnetic data from ships is not enough to perform a regional-scale analysis, so the global EMAG-2 (Maus *et al.*, 2009) database was used. This set has a spatial resolution of 2' arc (~ 3.7 km) and is based on data retrieved from multiple platforms with interpolation and correction at 3-4 km above the geoid.

Magnetic modeling

Synthetic magnetic anomalies

Magnetic anomalies of the deep seafloor generated by the spreading at the ridge were modeled after Vine & Matthews (1963) and corrected and interpreted according to the scale of magnetic polarity of Cande & Kent (1992, 1995). Synthetic anomalies were produced for a section north of the JFR, orthogonal to the magnetic pattern. This area was selected because of the

absence of the tectonic complexity observed in the southern part (*e.g.*, Selkirk trough). Parameters used for the best fit were: origin of the anomalies at 32°S, original azimuth of 0°, spreading rate of 6.6 cm yr⁻¹ and magnetic susceptibility of 0.005.

2.5D direct magnetic modeling

Direct modeling was performed with Geomodel© software for the Cinque Ports seamount as an example of typical isolated seamount in order to separate the effect of the seamount and magnetic fabric of the ocean floor. The N-S section starts at 33°S, run through the seamount and extends 170 km. A number of trials were performed with different geometry and values of magnetic susceptibility of the magnetic bodies below surface. Considering the non-unicity of the solutions for potential methods, magnetic thickness of the crust was set at ~ 1 km and bodies were created according to the interpreted features of the bathymetric and magnetic maps. Average magnetic susceptibility for basalts was used as done for the synthetic anomalies. Parameters of the magnetic field were considered as those from 2005, approximately the time of compilation of EMAG-2, including the datum of the magnetic compilation (3 km above sea level). Before, magnetic signatures were modeled for a prism and a cone in order to obtain anomalies from the ambient field. Lateral extension of the modeled bodies was 10 km (2.5D modeling), which

is in agreement with the typical width of magnetic anomalies in the base map.

3D inverse magnetic modeling

The 3D magnetic model was produced with an algorithm based on the 3D inversion procedure of Macdonald *et al.* (1980), which is based on the classic method of Parker (1973) and Parker & Huestis (1974) using Mirone (Luis, 2007). Resolution of the bathymetric grid was reduced to 2' in order to equal that of the EMAG-2. Parameters were used as for the 2.5D model and results were in reference to sea level for comparison purposes.

RESULTS

Morphology and lineaments

Despite the occurrence of individual seamounts and islands, the western segment of the JFR is a volcanic corridor with a common base at 3900 m depth (Figs. 2-3). This base is elongated in the $\sim 85^\circ\text{E}$ direction (Fig. 3) and hosts 22 summits, 15 of them with relevant elevation (>1000 m above the seafloor; Fig. 3). In addition, there is a secondary N-S trending elongation that corresponds to a prolongation of four seamount/islands clusters: Gamma and Beta with a length of 133.5 km and 90.7 km wide; Alfa and Robinson Crusoe with 110.2 km and 85.5 km, respectively; Duke, Cinque Ports and Dresden seamounts along with Alejandro Selkirk Island with 149 km and 65.7 km; and finally Friday and Domingo seamounts with a length of 69.8 km and a width of 44.8 km (Figs. 2, 3). Note that new seamount names have been introduced for better identification: Duke, which is the name of the ship that rescued Alejandro Selkirk in 1709 AD; Cinque Ports, which is the ship that left him in 1703 AD; and Dresden, the German ship sunken in Cumberland bay during the WW1.

There are additional seamounts on the seafloor in this area that depart from the main JFR (grey circles in Fig. 3) forming N-S trending alignments. Minor topographic lineaments (solid lines in Fig. 3) mostly identified in the multibeam bathymetry are orthogonal to the Nazca Plate vector displacement and probably represent a fabric developed at the East Pacific Rise. On the other hand, the trace of the Challenger Fracture Zone is clear in the SW area (Fig. 3) but diffuse to the north, especially between Robinson Crusoe Island and Duke Seamount.

Magnetic anomalies from EMAG-2

Figure 4 shows magnetic anomalies from EMAG-2 for the study area where the pattern acquired by seafloor

spreading is dominant. Values usually range between 200 and -200 nT with typical wavelengths of *ca.* 38.8 km. Some areas present higher values, especially close to the Challenger Fracture Zone, whose trace can be better recognized here than in bathymetric data. In fact, the trace (dashed line in Fig. 3) is characterized by an elongation of the magnetic anomalies in the $\sim \text{N}60\text{-}65^\circ\text{E}$ with low amplitude, a pattern that disrupts the regular fabric of the deep seafloor. Interestingly, the anomalies are deflected to the W in the southern area and to the E in the northern area of the JFR (Fig. 5). In addition, some magnetic dipoles are observed around the islands/seamounts with the highest values of magnetization, which could represent subvolcanic bodies that can be identified through the 2.5D modeling.

Magnetic anomalies by seafloor spreading

Isochrones for synthetic anomalies are shown in Figure 6a for the A-B section (Fig. 5). Figure 6b shows observed anomalies that are correlated with the modeled anomalies and Figure 6c represents the model with age and magnetic polarities. Ages in the northern part range from ~ 25.8 and ~ 36.6 Myr, which are slightly older than those of the southern part where ages range from ~ 22 and ~ 36 Myr.

2.5D model for Cinque Ports Seamount

Modeling for the Cinque Ports seamount was performed as an attempt to identify volcanic structures. Despite the bathymetric expression of this seamount, the model suggests a composed magnetic source where both seafloor and seamount magmatic rocks contribute to the signal (Fig. 7, Table 1). Limits of the modeled units could correspond to minor structures (fractures or faults) but the space between unit 5 and 6 could represent the fracture zone.

3D magnetization model

The Challenger Fracture Zone is notably observed in the 3D magnetization model (dashed line in Fig. 8), which marks the relative displacement of the seafloor anomalies from south to north of the JFR. Magnetization values range from -5 to 5 A m^{-1} with the highest related to the islands and mostly along the edge of the fracture zone. They are not centered on the seamount summits and do not follow the trend of bathymetry (Fig. 8).

DISCUSSION

The interpretation of the magnetic data helps to us understand the tectonic evolution of the seafloor and its structures. The existence of ridges, microplates and other

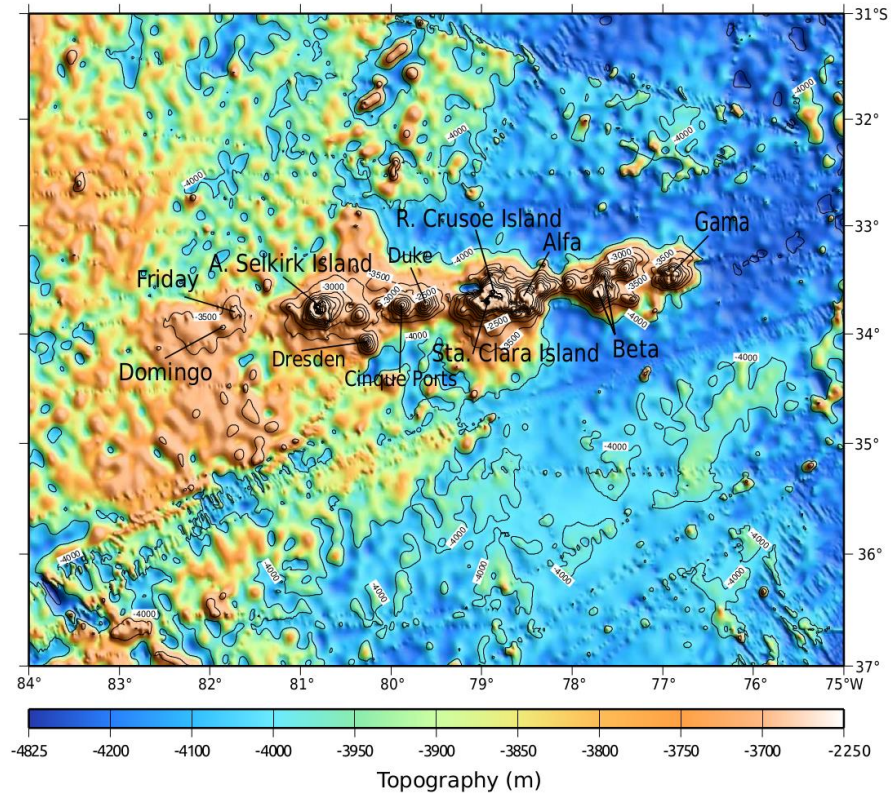


Figure 2. Map of the submarine topography. Bathymetric contours every 500 m. The names of the islands (see text for details) and main seamounts are shown.

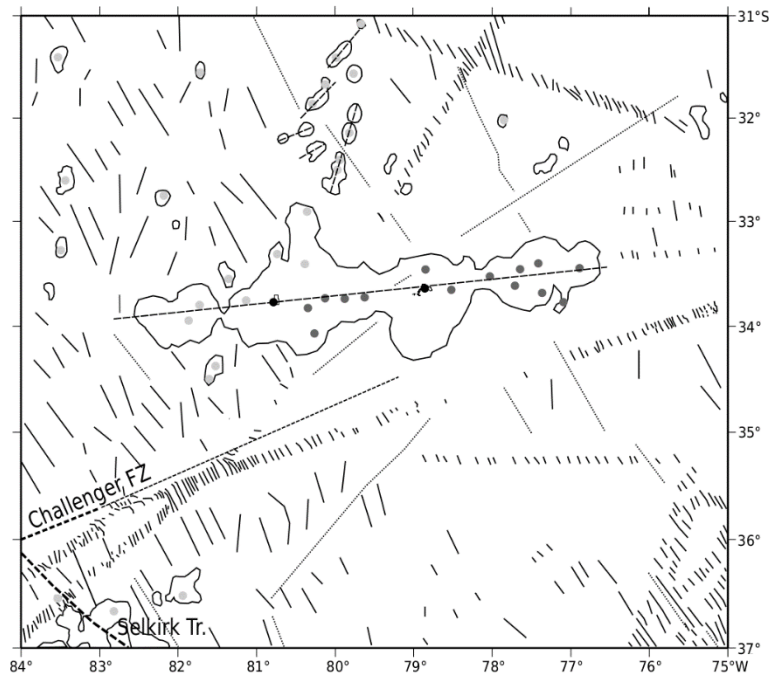


Figure 3. Map of seafloor lineaments (solid lines), Juan Fernández Ridge and other submarine elevations (long segmented line), trace of the Challenger Fracture Zone and Selkirk Depression, minor depressions (dotted lines), position of the islands (black circles), and position of the major (dark gray circles) and minor summits (light gray circles). Topographic base contour of the ridge is also shown.

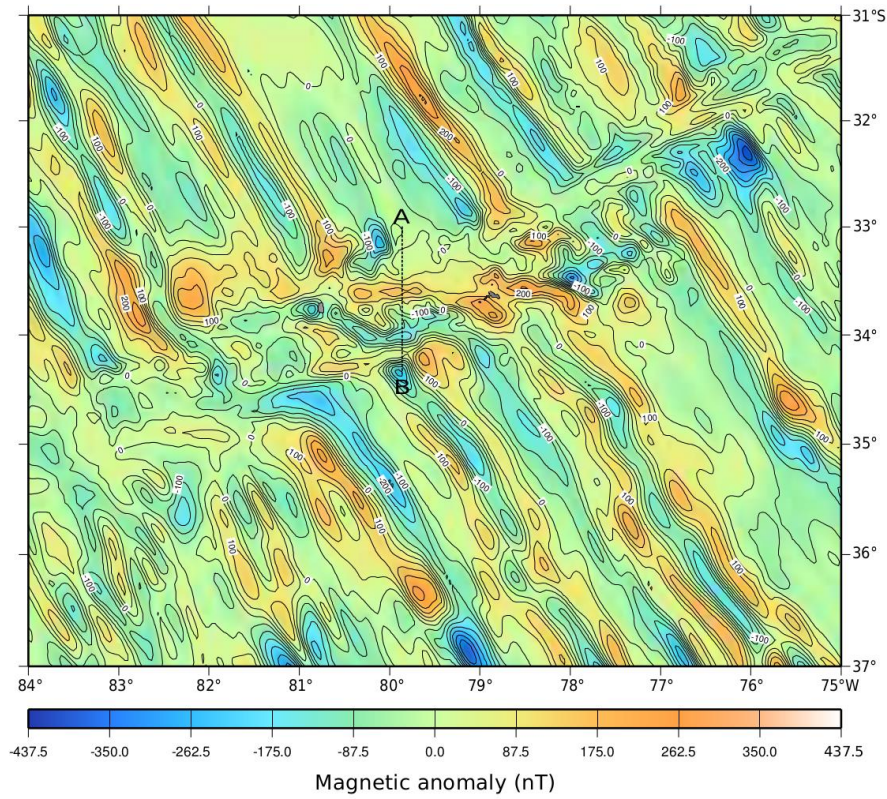


Figure 4. Map of magnetic anomalies. Magnetic contours every 25 nT. The location of the section A-B for the direct magnetic modeling is indicated.

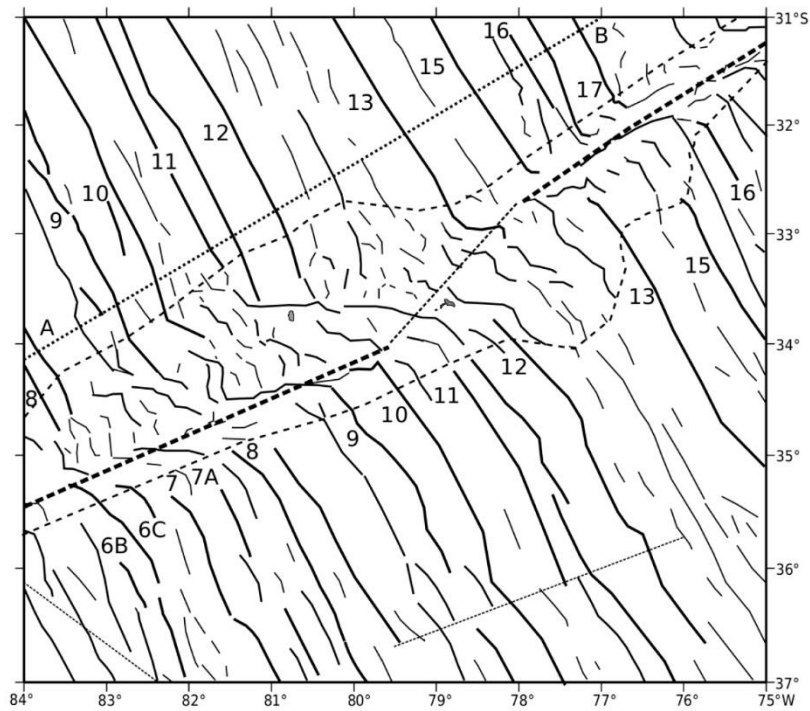


Figure 5. Interpretation map of the magnetic anomalies. Major magnetic lineaments with solid thick line; secondary ones with thin line. The trace of the Challenger Fracture Zone is shown with thick and thin dashed lines. Dashed narrow lines show anomaly offsets. Long and thin dashed lines indicate the area of deformation of the magnetic anomalies. Location of the A-B section for synthetic magnetic anomalies is also indicated.

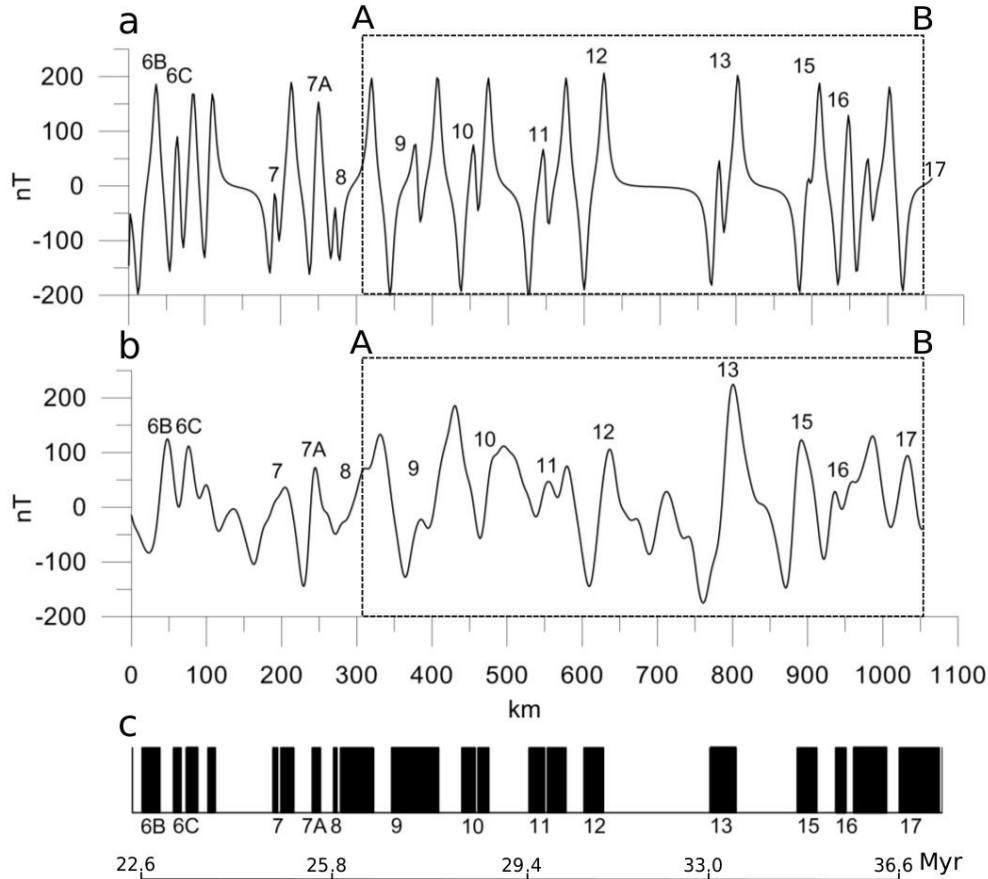


Figure 6. a) Synthetic magnetic anomalies for A-B section (Fig. 5). Isochrones are shown, b) observed magnetic anomalies for A-B section (Fig. 5), c) block model of magnetic polarities and ages.

other fossil structures, changes of seamount tracks, fractures and other lineaments, is evidence of the complicated past of the South Pacific. Observed discontinuities and distortions of the magnetic lineaments and interpretations are consistent with the seafloor tectonic evolution proposed by Tebbens *et al.* (1997) and Tebbens & Cande (1997), including the crust velocity expansion of 6.6 cm yr^{-1} for the study area (*e.g.*, Gordon & Jurdy, 1986; Cande & Haxby, 1991).

The magnetic fabric in the area is dominated by features common in the East Pacific Rise but the departure of JFR from the magnetic fabric of the seafloor is remarkable. The Challenger Fracture Zone introduces a remarkable distortion on this pattern and JFR appears as a subtle superimposed signal. It also produces a diminution of the magnetic amplitudes. The JFR is located inside of the magnetic deformation zone and, in fact, no important seamounts or structural highs are identified outside of this zone. On the other hand, some small-scale features, such as the presence of seafloor older than 6C isochrone close to the intersection between Challenger Fracture Zone and the

Selkirk trough, suggest a more complex tectonic history (and possible formation of Selkirk microplate before 24–25 Myr). In addition, the dissected pattern of magnetic fabric in the south-eastern area suggests an unknown tectonic history and/or presence of fractures zones not yet recognized.

A relevant difference between the eastern cluster (O'Higgins Seamount and Guyot) (Von Huene *et al.*, 1997; Yáñez *et al.*, 2001) and the segment analyzed here is that the latter does not show such a clear magnetic signature of isolated bodies. On the contrary, a superposition of magnetic sources arises, some of them departing from the general trend of the JFR and without direct correlation with the bathymetric features. The Challenger Fracture Zone, whose trace across the JFR is clearer in the magnetic data, distorts the magnetic fabric of the seafloor and seems to control the presence of magmatic intrusions beyond the trend of the JFR (see conceptual model of Fig. 9), which would have been a leakage structure under appropriate conditions. Thus, one can speculate that plate tectonic processes have played a role in controlling magma ascent

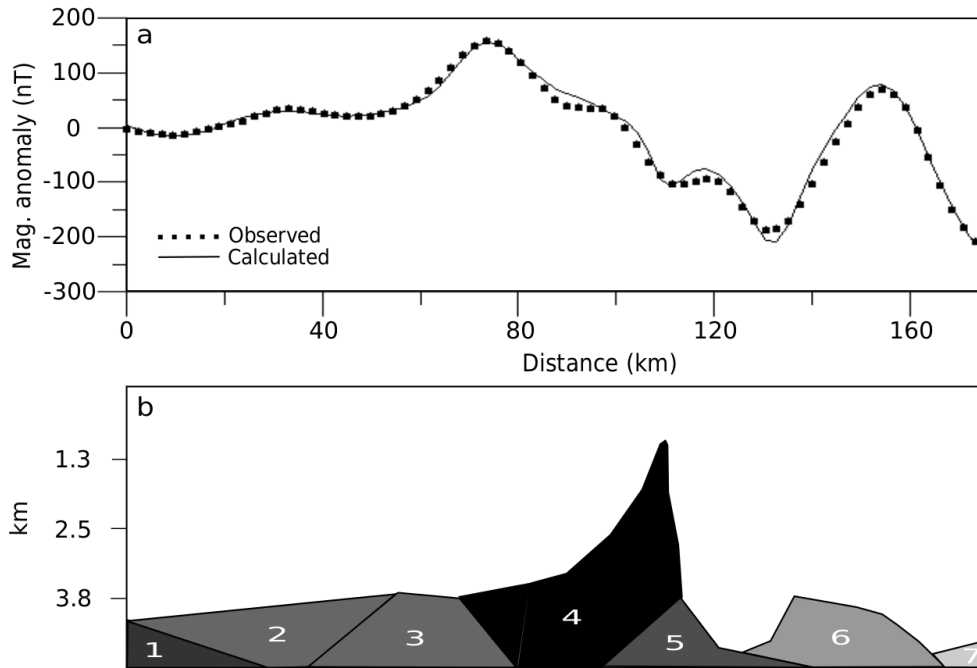


Figure 7. 2.5D direct magnetic model (location of A-B section in Fig. 4). a) Fit between observed and calculated magnetic anomalies is shown, b) model and resulting magnetic bodies. North is on the left.

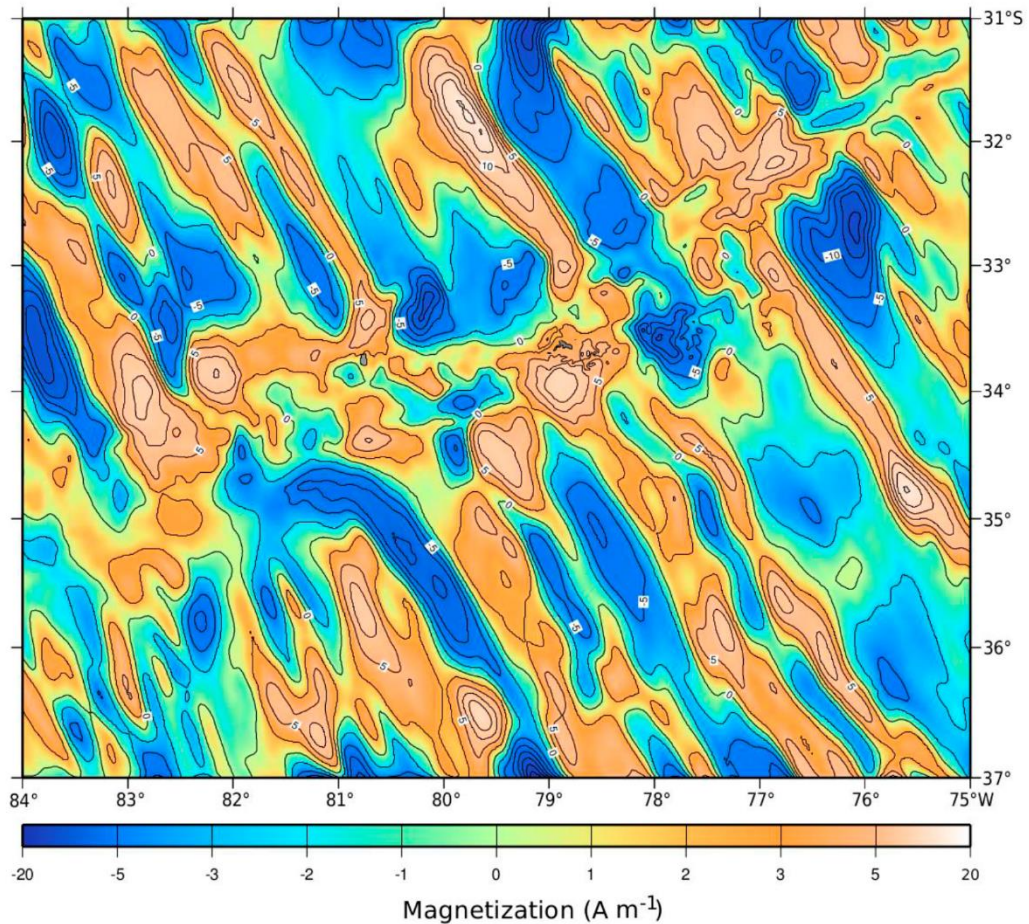


Figure 8. 3D magnetization model map. Contours every 2.5 $A\ m^{-1}$.

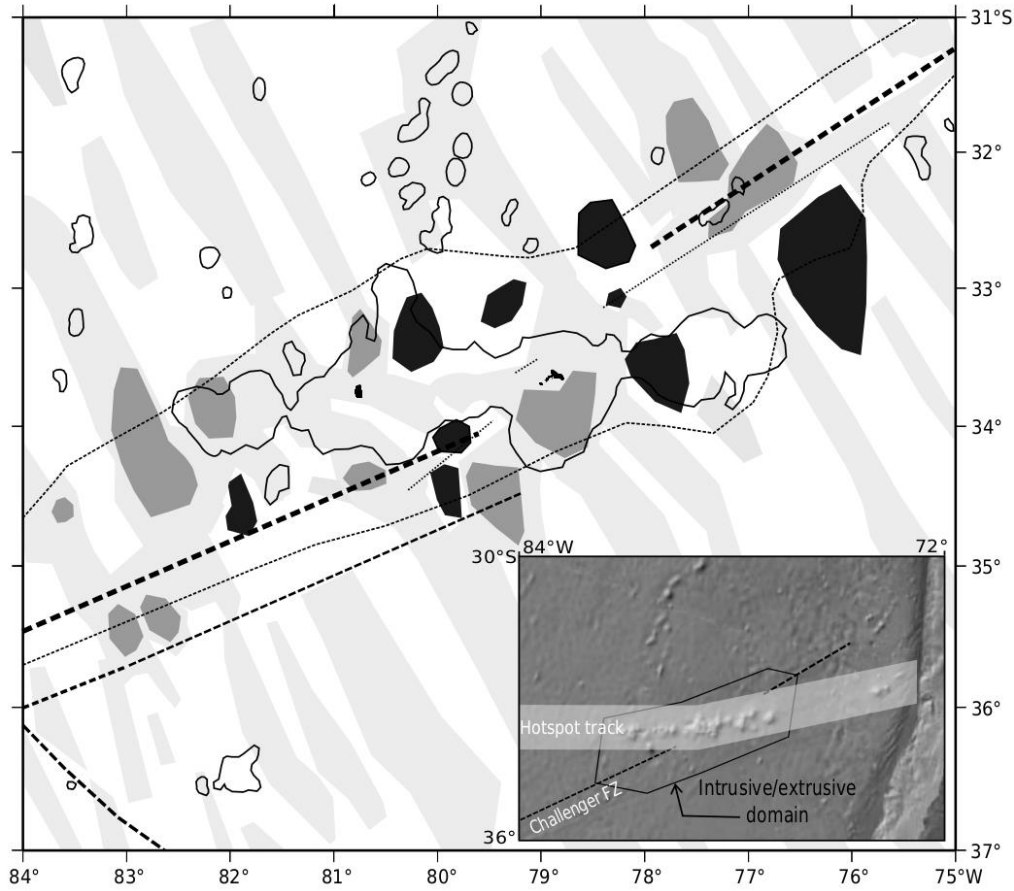


Figure 9. Interpretation map of the magnetization pattern. Light gray areas indicate blocks of oceanic crust with normal polarity. Intermediate gray areas correspond to sectors with higher positive values of magnetization in the area of deformation of the magnetic lineaments, and those with darker gray, negative magnetization (see Figs. 3 and 5 for further details). Box shows a conceptual model for the situation.

Table 1. Magnetic susceptibility for the 2.5D modeled bodies (Fig. 7).

Bodies	Susceptibility (SI)
1	0.009
2	0.011
3	0.012
4	-0.003
5	0.010
6	0.045
7	0.063

ascent and arrest from both the fixed mantle plume (seamounts and islands along the main JFR corridor) and perhaps the upper mantle (peripheral and/or isolated seamounts or intracrustal intrusions).

CONCLUSIONS

A remarkable feature that characterizes the western segment of the JFR is that seamounts and islands form a platform with a common base at 3500 m depth from Alejandro Selkirk Island to Gamma seamount. The Friday and Domingo Seamounts form a cluster with a base at ~3900 m, connected to the platform. A section of deep ocean floor separates this western segment from the O'Higgins cluster. On the other hand, the magnetic fabric is dominated by the seafloor pattern, with a distortion caused by the Challenger Fracture Zone that separates a northern area with older seafloor ages. The western (younger) JFR ridge segment appears as a superimposed feature embedded in a more prominent east-northeast trend of magnetization of the seafloor, which in turn cuts the deep seafloor fabric. Opposite to that observed for the O'Higgins Seamount on the east, the magnetic signature on the western segment, and especially along the Challenger Fracture

Zone, does not correlate strictly with bathymetry and cannot be explained by isolated bodies with a common polarity. On the contrary, evidence suggests a superposition of magnetic sources; some of them related to seamounts and islands, others related to the structural pattern and potentially represent subsurface intrusions of different ages.

We have presented concurrent evidence of a structural pattern that suggests the Challenger Fracture Zone is a channel for magmatic intrusions. This fuels the discussion about the competing role of mantle plumes and tectonic processes. Our findings suggest that mantle plume processes seem to exert a first-order control on the modern JFR architecture but plate tectonic processes have also played a secondary role.

ACKNOWLEDGEMENTS

Data modeling effort was supported by Fondecyt 1110966 grant to L.E.L. Magnetic data is acknowledged to Cooperative Institute for Research in Environmental Sciences (CIRES, University of Colorado-NOAA) and global bathymetry was taken from Scripps Institution of Oceanography, University of California. GMT software was used for some figures and Mirone for inverse modeling (J.F. Luis). Geomodel© software was downloaded from the G.F.J. Cooper website, University of the Witwatersrand, Johannesburg. Journal reviewers are kindly acknowledged by their constructive criticism.

REFERENCES

- Anderson, D.L. 2013. The persistent mantle plume myth. *Aust. J. Earth Sci.*, 60(6-7): 657-673. doi: 10.1080/08120099.2013.835283.
- Andrade, I. & G. Pequeño. 2008. Mesobathic Chondrichthyes of the Juan Fernández seamounts: are they different from those of the central Chilean continental slope? *Int. J. Trop. Biol. Conserv.*, 56: 181-190.
- Arana, P. 1985. Investigaciones marinas en el archipiélago de Juan Fernández. Escuela de Ciencias del Mar, Universidad Católica de Valparaíso, Valparaíso, 308 pp.
- Arana, P. 2010. La isla de Robinson Crusoe. Ediciones Universitarias de Valparaíso, Valparaíso, 308 pp.
- Batiza, R. 1982. Abundances, distribution and sizes of volcanoes in the Pacific Ocean and implications for the origin of non-hotspot volcanoes. *Earth Planet. Sci. Lett.*, 60: 195-206.
- Becker, J.J., D.T. Sandwell, W.H.F. Smith, J. Braud, B. Binder, J. Depner, D. Fabre, J. Factor, S. Ingalls, S.H. Kim, R. Ladner, K. Marks, S. Nelson, A. Pharaoh, R. Trimmer, J. Von Rosenberg, G. Wallace & P. Weatherall. 2009. Global bathymetry and elevation data at 30 arc seconds resolution: SRTM30 PLUS. *Mar. Geod.*, 32: 355-371.
- Blais, A., P. Gente, M. Maia & D.F. Naar. 2002. A history of the Selkirk Paleomicroplate. *Tectonophysics*, 359: 157-169.
- Bonatti, E.C., G.A. Harrison, D.E. Fisher, J. Honnorez, J.G. Schilling, J.J. Stipp & M. Zentilli. 1977. Easter volcanic chain (southeast Pacific): a mantle hot line. *J. Geophys. Res.*, 82: 2457-2478.
- Cande, S.C. & W.F. Haxby. 1991. Eocene propagating rifts in the southwest Pacific and their conjugate features on the Nazca Plate. *J. Geophys. Res.*, 96: 148-227.
- Cande, S.C. & D.V. Kent. 1992. A new geomagnetic polarity time scale for the Late Cretaceous and Cenozoic. *J. Geophys. Res.*, 97: 13917-13951.
- Cande, S.C. & D.V. Kent. 1995. Revised calibration of the geomagnetic polarity timescale for the Late Cretaceous and Cenozoic. *J. Geophys. Res.*, 100: 6093-6095.
- Clark, M., A.A. Rowden, T. Schlacher, A. Williams, M. Consalvey, K.I. Stocks, A.D. Rogers, T.D. O'Hara, M. White, T.M. Shank & J.M. Hall-Spencer. 2010. The ecology of seamounts: structure, function, and human impacts. *Ann. Rev. Mar. Sci.*, 2: 253-278.
- Clouard, V. & A. Bonneville. 2001. How many Pacific hotspots are fed by deep-mantle plumes? *Geology*, 29: 695-698.
- Courtillot, V., A. Davaille, J. Besse & J. Stock. 2003. Three distinct types of hotspots in the Earth's mantle. *Earth Planet. Sci. Lett.*, 205: 295-308.
- Davies, D.R. & J.H. Davies. 2009. Thermally-driven mantle plumes reconcile multiple hot-spot observations. *Earth Planet. Sci. Lett.*, 278: 50-54.
- DeMets, C., R.G. Gordon, D.F. Argus & S. Stein. 1994. Effect of recent revisions to the geomagnetic reversal time scale on estimates of current plate motions. *Geophys. Res. Lett.*, 21: 2191-2194.
- Devey, C.W., C. Hemond & P. Stoffers. 2000. Metasomatic reactions between carbonated plume melts and mantle harzburgite: the evidence from Friday and Domingo seamounts (Juan Fernandez chain, SE Pacific). *Contrib. Mineral. Petrol.*, 139: 68-84.
- Farley, K.A., A.R. Basu & H. Craig. 1993. He, Sr, and Nd isotopic variations in lavas from the Juan Fernández Archipelago, SE Pacific. *Contrib. Mineral. Petrol.*, 115: 75-87.
- Foulger, G.R. 2011. *Plates vs Plumes: a geological controversy*. Wiley-Blackwell, New York, 364 pp.
- Gordon, R.G. & D.M. Jurdy. 1986. Cenozoic global plate motions. *J. Geophys. Res.*, 91: 12389-12406.

- Handschumacher, D.W. 1976. Post-Eocene plate tectonics of the Eastern Pacific. In: G.H. Sutton, M.H. Mangnani & R. Moberly (eds.). *The Geophysics of the Pacific Ocean Basin and its margin*. Amer. Geophys. Union, Geophys. Monogr., 19: 177-202.
- Hey, R. 1977. A new class of "pseudofaults" and their bearing on the plate tectonics: a propagating rift model. *Earth Planet. Sci. Lett.*, 37: 321-325.
- Kopp, H., E.R. Flueh, C. Papenberg & D. Klaeschen. 2004. Seismic investigations of the O'Higgins Seamount Group and Juan Fernández Ridge: aseismic ridge emplacement and lithosphere hydration. *Tectonics*, 23(2), doi: 10.1029/2003TC001590.
- Koppers, A.A., P.H. Staudigel, M.S. Pringle & J.R. Wijbrans. 2003. Short-lived and discontinuous intraplate volcanism in the South Pacific: Hot spots or extensional volcanism? *Geochem. Geophys. Geosys.*, 4(10): 1089, doi: 10.1029/2003GC000533.
- Koppers, A.A.P. & A.B. Watts, 2010. Intraplate seamounts as a window into deep earth processes. *Oceanography*, 23: 42-57.
- Luis, J.F. 2007. Mirone: a multi-purpose tool for exploring grid data. *Comp. Geosci.*, 33: 31-41.
- Macdonald, K.C., S.P. Miller, S.P. Huestis & F.N. Spiess. 1980. Three-dimensional modeling of a magnetic reversal boundary from inversion of deep-tow measurements. *J. Geophys. Res.*, 85: 3670-3680.
- Mammerickx, J. & K.D. Klitgord. 1982. Northern East Pacific Rise: evolution from 25 m.y. B.P. to the present. *J. Geophys. Res.*, 87: 6751-6759.
- Matthews, K.J., R.D. Müller, P. Wessel & J.M. Whittaker. 2011. The tectonic fabric of the ocean basins. *J. Geophys. Res.*, 116: B12109, doi:10.1029/2011JB008413.
- Maus, S., U. Barckhausen, H. Berkenbosch, N. Bournas, J. Brozena, V. Childers, F. Dostaler, J.D. Fairhead, C. Finn, R.R.B. von Frese, C. Gaina, S. Golynsky, R. Kucks, H. Lühr, P. Milligan, S. Mogren, R.D. Müller, O. Olesen, M. Pilkington, R. Saltus, B. Schreckenberger, E. Thébaud & F. Caratori-Tontini. 2009. EMAG2: a 2-arc min resolution Earth Magnetic Anomaly Grid compiled from satellite, airborne, and marine magnetic measurements. *geochem. geophys. geosys.*, 10: Q08005.
- Menard, H. 1964. *Marine geology of the Pacific*. Mc Graw-Hill, New York, 271 pp.
- Morgan, W.J. 1971. Convection plumes in the lower mantle. *Nature*, 230: 42-43.
- Parker, R.L. 1973. The rapid calculation of potential anomalies. *J. Roy. Astr. Sci.*, 31: 447-455.
- Parker, R.L. & S.P. Huestis. 1974. The inversion of magnetic anomalies in the presence of topography. *J. Geophys. Res.*, 79: 1587-1593.
- Pilger, R.H. 1981. Plate reconstructions, aseismic ridges, and low-angle subduction beneath the Andes. *Geol. Soc. Am. Bull.*, 92: 448-456.
- Smith, W.H.F. & D.T. Sandwell. 1997. Global seafloor topography from satellite altimetry and ship depth soundings. *Science*, 277: 1956-1962.
- Steinberger, B. 2000. Plumes in a convecting mantle: models and observations for individual hotspots. *J. Geophys. Res.*, 105: 11127-11152.
- Tebbens, S.F. & S.C. Cande. 1997. Southeast Pacific tectonic evolution from early Oligocene to Present. *J. Geophys. Res.*, 102: 12061-12084.
- Tebbens, S.F., S.C. Cande, L. Kovacs, J.C. Parra. J.L. LaBrecque & H. Vergara. 1997. The Chile Ridge: a tectonic framework. *J. Geophys. Res.*, 102: 12035-12059.
- Vergara, H. & E. Morales, 1985. Morfología submarina del segmento central del cordón asísmico Juan Fernández. In: P. Arana (ed.). *Investigaciones marinas en el archipiélago de Juan Fernández*. Universidad Católica de Valparaíso, Valparaíso, pp. 25-34.
- Vine, F. & D.H. Matthews. 1963. Magnetic anomalies over oceanic ridges. *Nature*, 199: 947-949.
- Von Huene, R., J. Corvalán, E.R. Flueh, K. Hinz, J. Korstgard, C.R. Ranero & W. Weinrebe. 1997. Tectonic control of the subducting Juan Fernández Ridge on the Andean margin near Valparaíso, Chile. *Tectonics*, 16: 474-488.
- Wilson, J.T. 1965. Evidence from ocean islands suggesting movement in the earth. *Trans. Roy. Soc.*, 258: 145-167.
- Yáñez, G.A., C.R. Ranero, R. Von Huene & J. Díaz. 2001. Magnetic anomaly interpretation across the southern central Andes (32°-34°S): the role of the Juan Fernández Ridge in the late Tertiary evolution of the margin. *J. Geophys. Res.*, 106: 6325-6345.
- Yáñez, G.A., J. Cembrano, M. Pardo, C. Ranero & D. Selles. 2002. The Challenger-Juan Fernández-Maipo major tectonic transition of the Nazca-Andean subduction system at 33°-34,8°S: geodynamic evidence and implications. *J. S. Am. Earth Sci.*, 15: 23-38.